

# Large bandwidth identification of a rotor model

J-J. Costes \*

ONERA DDSS/CA

BP 72 – 29 avenue de la division Leclerc. 92322 CHATILLON Cedex  
FRANCE

\* e-mail address : [jj.costes@onera.fr](mailto:jj.costes@onera.fr)

## 1. INTRODUCTION

The active control of the helicopter rotor is a challenging task. The objective is to use the response of transducers located on the blades and on the fuselage to compute commands in order to reduce the vibrations of the whole structure. As a first step towards this objective, we have the identification of the rotor. By identification, it is intended the modeling of the response of the transducers to the command inputs. This task presents unusual difficulties as the rotor in rotation is a periodic system and moreover the vibratory environment is very noisy. At ONERA, we have attempted the identification of a 3 bladed rotor model in hover by different methods. Only one method has given reliable results. This method will be detailed here.

## 2. OVERALL DESCRIPTION OF THE EXPERIMENT.

The model, named EDY, is a 3 bladed rotor articulated in flap. The diameter of the rotor is 1,65m. The blades are rigid in the lead-lag direction. The blades pitch angles are determined by the position of a swash plate. The swash plate position is set by 3 hydraulic actuators. The rotor is mounted on top of a relatively rigid and heavy body. For better security, this body is fastened to the ground by means of rigid struts.

A preliminary experiment (in hover) took place at ONERA in the BRAVoS test rig in May 1999. The aim of the study was to test the rotor model and try an identification in the time domain. Of particular interest was the spectrum of the output responses and the identification of the modes. During the experiment, the rotational speed was set at 200, 400 or 600 rpm. The mode frequencies are reported in figure 1 as a function of the rotational speed. In this figure, one can note a "rigid flap" mode, the frequency of which is roughly equal to

the rotational frequency of the rotor. This is what is expected for an articulated rotor. We have also a "flexible flap" mode and 2 other body modes which are only detected by the accelerometers placed on the non rotating structure. In figure 1, the shaded areas correspond to high frequencies where no measurements were possible because of the acquisition frequency (Shannon condition) or simply because the level of the response was too low. Several methods of identification have been tried([1]....[4]). Only the one that will be detailed later has proved to be reliable.

Though the experiment of May 1999 was largely satisfactory, it also appeared that the bandwidth allowed for the output responses was too limited. So in September 2000, another experiment was performed in the same test rig. As for the previous experiment, the excitation of the model is done by means of the three actuators which set the swash plate position. As these actuators were not designed for unsteady work, they cannot be operated at a frequency greater than 100 Hertz, to avoid instabilities into the hydraulic system. This condition is fulfilled by having the three input signals to pass through a low-pass filter before they are transmitted to the actuators. Nevertheless, the signals coming from the output transducers are recorded at a much higher frequency. Only one kind of identification has been performed. The method of identification is the extension of an existing method by Mäkilä (references [3] [4]) to the case of periodic systems. The mathematical developments are presented in paragraph 4. The present paper will show the new results for a unique speed of rotation of the rotor as well as two tests to check for the accuracy of the identifications.

The model, as it is identified, cannot be used for the development of a feed-back control loop by classical methods because the parameters are much too numerous for Linear Quadratic (LQ) or Linear Quadratic Gaussian (LQG)

regulators. Nevertheless the identification can be used in LMS (Least Mean Square) or IMC (Internal Model Control) approaches and also for the design of a controller by trial and error as in reference [5].

The rotational speed is 400 rpm in the September 2000 experiment. The 200 and 400 rpm cases have not been considered this time and the outputs of the accelerometers on the non rotating structure have not been recorded. The maximum variation of the blade pitch angle is 1. degrees. The mean pitch angle is 0. degree. The signals recorded during the experiment may be arranged in 2 groups. The first group is composed of signals coming from the rotor. We have for the first group a total of 9 signals

<i>Transducer</i>	<i>Channel number</i>
Angle transducer on blade 1	Channel 1
Angle transducer on blade 2	Channel 2
Angle transducer on blade 3	Channel 3
Strain gauge at blade root, blade 1	Channel 4
blade 2	Channel 5
blade 3	Channel 6
Strain gauge, mid distance from tip, blade 1	Channel 7
blade 2	Channel 8
blade 3	Channel 9

These 9 signals are coming from rotating parts of the structure, they are radio-transmitted to the recording apparatus. The radio transmission is done as follow :

The analog signal coming from a transducer is first discretized at a very high frequency, it is then filtered by a low pass filter whose cutting frequency is 1000 Hz. The digitized values are transmitted by radio waves for recording and further treatment. After the radio transmission, the signals are discretized again and this time at a frequency of 5000 Hz. This is a much higher than necessary frequency because the signals cannot contain frequency components over 1000 Hz. The reason for the use of such a high frequency will be explained later.

A second group of signals comes from non rotating transducers

<i>Transducer</i>	<i>Channel number</i>
Displacement transducer on : actuator a	Channel 10
actuator b	Channel 11
actuator c	Channel 12

<i>Transducer</i>	<i>Channel number</i>
Input signal into : actuator a	Channel 13
actuator b	Channel 14
actuator c	Channel 15
instantaneous rotational speed	Channel 16

The input signals are coming from independent random generators and are thus uncorrelated. The signals are filtered by analog low pass filters, the cutting frequency of these filters is 100 Hz to avoid instability problems with the hydraulic actuators. As the signals in the second group are in the non rotating frame, they don't go through the radio transmitter. They are directly discretized 5000 times by second. The choice of 5000 Hz for the sampling frequency is now explained :

The azimuthal position of the rotor blades must be defined. This is done by having a rectangular signal of duration 500  $\mu$ s to be generated each time the blade number 1 passes at azimuth zero, the reference azimuth. For a speed of rotation of 400 rpm, the azimuth of the blades has changed by 1.2 degrees in 500  $\mu$ s . At the frequency of 5000 Hz , we have a record every 0.48 degree. Thus, the rectangular signal cannot be missed. We have at least 2 points and at most 3 points during the time interval of 500  $\mu$ s. In any case, the phase error introduced by the sampling is less than 0.48 degree and it can be neglected. The total recording time is 540 s which corresponds to 3600 rotations when the speed of rotation is 400 rpm. Nevertheless the speed of rotation varies by some amount during the experiment and 3600 rotations is only an approximate value. The rotational speed remains into the interval 380 to 420 rpm. The high sampling frequency is needed for the capture of the rectangular signal at azimuth zero but the lot of data generated is unnecessarily large. Only 60 samples by rotation are saved for further analysis. This corresponds to a final sampling frequency of 400 Hz and allows a Fourier analysis of the signals up to 200 Hz.

During the experiment of May 1999, the signals coming from the different transducers were recorded 15 times by rotation at 400 rpm. There was no need for a pre-sampling at high frequency because the specially designed electronics was able to react to the rising hedge of the rectangular signal. The experiment, as done in September 2000, is easier to perform and less prone to errors which may be introduced by custom made electronics. It also allows higher frequencies to be considered. Nevertheless, contrary to the May 1999 experiment, the azimuthal reference can only be obtained by an "off line" processing of the rectangular signal at azimuth zero.

### 3. POWER SPECTRUM ANALYSIS OF THE RECORDED SIGNALS.

The main purpose of the study is the identification of the model in the time domain. In the time domain the analysis of a structure with rotating parts is simpler. Nevertheless, much knowledge can be gained by a more classical analysis in the frequency domain.

#### 3.1 Power spectra of the input signals and of the actuator responses.

As was said earlier, the input signals are coming from independent random generators and they are filtered to avoid instabilities into the hydraulic command chain. The power spectra of the signals which are actually fed into the hydraulic actuators is presented in figure 3. The power spectra are not exactly alike but there is no signal over 100 Hz (reduced frequency 0.5)

Figure 4 (Channels 10, 11, 12) shows the response of the hydraulic actuators. On all these channels the limitation in frequency is evident but all the spectrums are different. This is due to the fact that the generators, as well as the actuators are alike but different apparatus.

Another remark may be done, on Channel 16, the instantaneous rotational speed was recorded and the power spectrum doesn't show peaks excepted at very low frequencies. Thus we can conclude that the body and blades flapping modes, with relatively high frequencies, have no effect on the rotor speed. Most probably the variation in speed comes from the electric motor itself and its automatic speed control.

#### 3.2 Resonant frequencies of the model.

Figure 1, obtained in May 1999, shows the evolution of the resonant frequencies of the model as a function of the rotational speed. In figure 1 one can note at 400 rpm a total of 4 resonant frequencies (6.7 Hz, 16., 30. and 38 Hz). The frequencies at 16. and 30 Hz have been seen only by the accelerometers on the body. They will not appear in the September 2000 experiment as we have no accelerometer this time. Figure 4, obtained during the September 2000 experiment shows the averaged power spectra (disregarding azimuthal position) of the channels 1 to 12 when the excitation of the model is done by the 3 hydraulic actuators fed by uncorrelated input signals. The variation of the pitch angles are random with a maximum of  $\pm 1$  degree around a mean angle equal to 0 degree. On the abscissa the normalized frequency is recorded. For the normalization, the frequency is multiplied by 2 and divided by the sampling frequency which is here 400 Hz, as was explained previously. The highest frequency which can be detected is thus 200 Hz. Frequencies over 200 Hz would be a problem by effect of aliasing but as

was said earlier, the recording frequency is 5000 Hz before sampling at 400 Hz. Thus a mathematical filtering is possible before the 400 Hz sampling. In any case figures 3, 4 and 5 show no frequency over 160 Hz. This is in agreement with the fact that there is no excitation over 100 Hz.

On channels 1 to 9, three resonant frequencies are conspicuous, at 6.66 Hz, 41.66 Hz and 122.71 Hz. At 6.66 Hz, we have obviously the first rigid flap, the frequency of which is equal to the rotational frequency of the rotor. The second frequency, around 41 Hz, corresponds to the first flexible flap which was detected with some uncertainty in the May 1999 experiment. Let us now speak of the third frequency at 122.7 Hz. This frequency appears on the response of the strain gauges located at the blade root and to a lesser extent, into the response of the strain gauges located at mid distance to the tip. This frequency is entirely absent from the response of all the other transducers, even from the angle-transducers. Thus, this frequency corresponds to a mode of deformation of the blades. This resonant frequency does not seem to have been encountered so far.

The power spectra of the signals coming from the channels 10 to 15 also show that there is no excitation at frequencies over 120 Hz. Nevertheless we have a very large response on channels 4, 5 and 6 at 122 Hz. So, according to the classical theory of unvarying systems, this mode should be unstable or close to instability. Of course, here the system is a periodic one and it is possible, by modulation with the frequency of rotation, to obtain excitations and responses outside the range of frequencies of the inputs. Another and probably most important source of excitation for the present rotor model is the looseness in the mechanical parts setting the blades pitch angles. This introduces shocks and then a large band excitation which can be considered as a kind of input noise. The frequency at 122 Hz may also be a third harmonic of the first flexible flap generated by some non linear process.

### 4. IDENTIFICATION OF THE MODEL.

#### 4.1 Theory.

The rotor model is a periodic system, the method used for the identification is presented below :

The identification is made by the method of Mäkilä (references [3] and [4]) for discretized systems. This method is restricted to the case of a single input / single output time invariant system. The system is modeled as a finite impulse response filter (FIR). The identified filter minimize the difference between experimental and computed cross-correlation functions of the input and output. Unstable modes cannot be modeled. This, in fact, is a great quality of the method because no spurious unstable modes can be introduced in modeling the data.

The method of Mäkilä must be extended to the case of a

multi-input / multi-output periodic system.

This task is accomplished in 3 steps :

- 1) Extension to the case of a multi-input, single output time independent discretized system.
- 2) Extension to the case of a multi-input, multi-output time independent discretized system.
- 3) Extension to the case of a discretized rotating system.

#### 4.1.1 Case of a multi-input, single-output system.

The system output  $y(t)$  is known at discretized instants  $t$ .  $y(t)$  is a  $1 \times 1$  scalar term and  $u(t)$  is a  $p \times 1$  column vector.

The inputs and the output are known at the same instants  $t \in \{0, \dots, n\}$

The auto-correlation functions  $\vartheta(k, l)$  and cross-correlation functions  $\phi(l)$  are also defined :

$$\vartheta(k, l) = \frac{1}{n+1} \sum_{t=0}^{t=n} u(t-k)u^T(t-l)$$

$$\phi(l) = \frac{1}{n+1} \sum_{t=0}^{t=n} y(t)u^T(t-l)$$

where by definition  $u(t)=0$  if  $t < 0$  and  $u^T(t)$  is the transpose of  $u(t)$ . The  $\vartheta(k, l)$  is a  $p \times p$  matrix, and  $\phi(l)$  is a  $1 \times p$  line vector.

The identified output signal  $\tilde{y}(t)$  is defined as :

$$\tilde{y}(t) = \sum_{k=0}^{k=N} a(k)u(t-k)$$

Where  $a(k)$  is a  $1 \times p$  line vector and  $k \in \{0, \dots, N\}$ .

The correlation function  $\tilde{\phi}(l)$  between the computed output  $\tilde{y}(t)$  and the inputs is also defined :

$$\tilde{\phi}(l) = \frac{1}{n+1} \sum_{t=0}^{t=n} \tilde{y}(t)u^T(t-l)$$

or 
$$\tilde{\phi}(l) = \frac{1}{n+1} \sum_{k=0}^{k=N} \sum_{t=0}^{t=n} a(k)u(t-k)u^T(t-l)$$

This may also be written as :

$$\tilde{\phi}(l) = \sum_{k=0}^{k=N} a(k)\vartheta(k, l)$$

Taking  $l \in \{0, \dots, M\}$ ,  $M+1$  functions  $\tilde{\phi}(l)$  can be defined.

We must now determine the coefficients of the  $N+1$  line vectors  $a(k)$  in such a way as to minimize the cost function  $J$ .

$$J = \sum_{l=0}^{l=M} |\phi(l) - \tilde{\phi}(l)|^2$$

The problem is the choice of the norm to be used for  $[\phi(l) - \tilde{\phi}(l)]$ . The most natural choice is the spectral norm because, for a multi-input / multi-output system, the  $\phi(l)$  and  $\tilde{\phi}(l)$  are rectangular matrices. Unfortunately, computation of a spectral norm would lead to a strongly non linear problem. Here, taking advantage that the  $\phi(l)$  and  $\tilde{\phi}(l)$  are line vectors, the Euclidean norm will be used instead :

$$J = \sum_{l=0}^{l=M} [\phi(l) - \tilde{\phi}(l)][\phi(l) - \tilde{\phi}(l)]^T$$

The optimum is reached when the derivatives of  $J$  with respect to the elements  $a(k)$  are equal to zero. This optimum is a minimum because  $J$  is always positive and is a second order function in all the unknown coefficients.

Let us have :  $A(l) = \phi(l) - \sum_{k=0}^{k=N} a(k)\vartheta(k, l)$

and 
$$J = \sum_{l=0}^{l=M} A(l)A^T(l)$$

If  $a_{ij}$  is the element on column  $j$  of the line vector  $a(i)$ , we have :

$$\frac{\partial}{\partial a_{ij}} A(l)A^T(l) = 2A(l) \frac{\partial A^T(l)}{\partial a_{ij}} = 2 \frac{\partial A(l)}{\partial a_{ij}} A^T(l)$$

The derivation of  $A(l)$  gives :

$$\frac{\partial}{\partial a_{ij}} A(l) = \frac{-\partial a(i)}{\partial a_{ij}} \vartheta(i, l) = -[\text{ligne } j \text{ de } \vartheta(i, l)]$$

that will be written as :  $\frac{\partial}{\partial a_{ij}} A(l) = -\vartheta(i, l)_{j,*}$

Finally we obtain :

$$\frac{\partial J}{\partial a_{ij}} = \sum_{l=0}^{l=M} \left[ \phi(l) - \sum_{k=0}^{k=N} a(k)\vartheta(k, l) \right] \vartheta(i, l)_{j,*}^T = 0$$

This expression is linear in all the unknown coefficients  $a_{ij}$ , writing it for all possible values of  $i$  and  $j$ , a linear system is obtained.

The coefficients  $a_{ij}$ , solution to this system will minimize the cost function  $J$ .

The choice of  $N$  determines how far back in time we go to estimate the output  $y(t)$ . The number  $M$  determines the maximum shift in time in the computation of the cross-correlation functions. It is natural to choose  $M = N$ .

**Application :** The method, as it has been explained here is applied to a simple system with two inputs and one output. There is only two line matrices  $a(k)$  which are randomly determined. The input sequences are also randomly generated and the output is computed with the two  $a(k)$  matrices. Some amount of uncorrelated noise is also added to the output sequence.

The extended Mäkilä's method is applied to the noise corrupted output signal. In the computations the numbers

$M$  and  $N$  are set to 5, that is to say that 5 line matrices are identified. It has been verified that the 3 last ones have negligible coefficients in all cases. The inputs are supposed to be known without errors. It is thus possible to compute the output of the identified system. This signal can be compared to the true output and the difference between both signals is the remaining noise. It is then possible to compute the root mean square value (rms) of the remaining noise signal and make the ratio with the rms value of the uncorrupted output signal. Three calculations have been performed with time sequences of 1000 points, 3500 points and 7000 points and with various amount of noise. The obtained results are presented in the table below :

Sequence 1000p	Seq. 1000p	Sequence 3500p	Seq. 3500p	Sequence 7000p	Sequence 7000p
% of error before filtering	% of error after filtering	% of error before filtering	% of error after filtering	% of error before filtering	% of error after filtering
5.60%	0.56%	5.80%	0.16%	5.81%	0.17%
11.30%	1.12%	11.60%	0.32%	11.62%	0.34%
28.21%	2.80%	28.95%	0.81%	29.03%	0.86%
56.42%	5.60%	57.90%	1.62%	58.06%	1.72%
112.80%	11.20%	115.81%	3.23%	116.11%	3.44%
169.30%	16.80%	173.71%	4.85%	174.17%	5.16%
282.10%	28.04%	289.52%	8.09%	290.29%	8.60%
338.50%	33.65%	347.42%	9.70%	348.34%	10.32%
394.90%	39.26%	405.33%	11.32%	406.40%	12.04%

As may be seen on the table, with a sequence of 1000 points, the percentage of error is about 10 times lower after filtering. For the sequences of 3500 or 7000 points the percentage of error is about 33 times lower after filtering. This remains true, even when the uncorrelated noise signal is very large, 4 times more important than the true signal.

As the principle of the method is correlation to sort out noise, it is quite natural that results are better when the time sequences are longer. In our case, 3500 points were sufficient. The computations even show a very slight degradation of the results for 7000 points. This may be due to statistical variations in the input data.

For the september 2000 experiment the recording time

correspond to about 3600 rotations of the rotor. As will be explained latter, it is this number which must be considered for the application of the extended Mäkilä's method. Though the number of inputs will be very large (180 inputs), one may still hope a good filtering of the signals as the number of points for the time sequences remains always superior or equal to 3500.

#### 4.1.2 Case of a multi-output system.

Let us suppose we have  $q$  outputs. The theory of the preceding paragraph can be repeated. We can still define a matrix  $A(l)$  with  $q \times p$  dimensions instead of  $1 \times p$  dimensions. We have to minimize the function

$$J = \sum_{l=0}^{l=M} |A(l)|^2$$

with the problem of choosing a norm for the matrix  $A(l)$ . The usual spectral or Frobenius norms for matrices do not lead to simple computations. It is thus proposed to determine the  $q \times p$  matrices  $a(k)$  line by line, that is to say to consider the system with  $q$  outputs as  $q$  independent single output systems. The problem is thus broken down into  $q$  independent problems of the kind already treated in the preceding paragraph.

#### 4.1.3 Case of a periodic system.

It is a well established fact that a periodic system may be considered as a time invariant system when the variables are considered over one period. Let us make things more precise for a discretized periodic system. In the usual state-space formulation we have :

$$\begin{aligned} x(k+1) &= A(k)x(k) + B(k)u(k) \\ y(k) &= C(k)x(k) \end{aligned}$$

The system is periodic with period  $N$ , they are only  $N$  such matrices  $A(k)$ ,  $B(k)$  and  $C(k)$ . When the state equations are considered from one period to the next, one can write :

$$x(k+N) = A'(k)x(k) + B'(k) \begin{pmatrix} u(k) \\ u(k+1) \\ \vdots \\ u(k+N-1) \end{pmatrix}$$

for the following period we have :

$$x(k+2N) = A'(k)x(k+N) + B'(k) \begin{pmatrix} u(k+N) \\ u(k+N+1) \\ \vdots \\ u(k+2N-1) \end{pmatrix}$$

We can note that the matrices  $A'(k)$  and  $B'(k)$ , which are obtained by a composition of the elementary matrices  $A(k)$  and  $B(k)$ , are the same from one period to the next. Still we have  $N$  such matrices

$A'(k)$  and  $B'(k)$  ( $k \in \{1, \dots, N\}$ ) The periodic system can thus be considered as  $N$  time invariant systems allowing the computation of the outputs at azimuth time  $k$  from one period to the next. All the commands during the period must be considered.

## 5. APPLICATION OF THE EXTENDED MÄKILÄ'S METHOD TO THE ROTOR MODEL

In the September 2000 experiment, the signals are discretized 60 times by period of the rotor. So, each output signal is broken down into 60 signals. Because we have 3 independent actuators, each one being also broken down into 60 inputs, the total number of inputs is 180. For each channel, we have thus to consider 60 systems with 180 entries. Taking as example a strain gage on the blade, the identification is the determination of the matrices  $[a_i]$ . At a time  $n$ , the mathematical representation of the output  $y$ , arranged into a vector  $(y)$  with 60 elements, is given by the following formula :

$$(y)_n = \begin{bmatrix} a_0 \end{bmatrix} (u)_n + \begin{bmatrix} a_1 \end{bmatrix} (u)_{n-1} + \dots + \begin{bmatrix} a_p \end{bmatrix} (u)_{n-p}$$

*Eq(1)*

The dimension of the vector  $(u)$  is 180 in our case. The matrix  $[a_0]$  should be equal to zero or at least its norm should be small because the transmission of the command into the output signal is not instantaneous.

We have also to consider as many systems as we have output signals.

Mäkilä's extended method is a very powerful tool as it can separate the measured signals between one part correlated with the inputs and another not correlated part which is called noise. As was shown in 4.1.1 the theory gives a linear system which must be solved. The matrix part of the linear system depends only on the inputs and so it is common to all the outputs. The outputs have an action only on the second member of the system. It is thus possible to make the programming in such a way as to have all the outputs treated together. This save a lot of computation time. The treatment of an experimental case takes only a few minutes on a workstation.

As the analysis is an identification in the time domain, the result is a number of numerical matrices which may be used

for simulations but are not visually interpretable.

We thus have two problems with an identification in the form of equation (1). The first problem is how to display the result of the identification and the second is how to check the validity or accuracy of the identification. We will now address these two problems.

According to equation (1), the result of the identification is a series of matrices  $[a_i]$  allowing the computation of vector  $(y)$  when the time history of the inputs is known. The vector  $(y)$  represents the time history of the output during one rotation. Introducing  $(y)^T$  the transpose of vector  $(y)$ , it is easy to compute the time history of one selected physical output ; For example, the series  $(Y)_{0 \rightarrow n}^T$  represents the time history of the signal  $y$  from the time  $t = 0$  to the time  $t = n$ .

$$(Y)_{0 \rightarrow n}^T = ((y)_n^T, (y)_{n-1}^T, (y)_{n-2}^T, \dots, (y)_0^T)$$

The reconstructed signal can be compared to the original one coming from the experiment. The power spectra of both signals may be computed and displayed on the same picture. The values of the resonant frequencies and the amplitude of the power spectra at those frequencies are also easily compared.

The second problem is to test the value of the reconstruction. The power spectra allow a comparison between amplitudes but no phase information is available. Phase information is of prime importance for active control. We shall give two ways to compare the phase of the reconstructed signal with the phase of the experimental one. This notion of phase makes only sense for a fixed given frequency. So the comparison must be done for all the frequencies in the range of interest.

### 5.1 First tool to check validity of the results.

The first tool is a rather crude one but its interpretation is easy. As it is well known, problems are occurring in active control when the phase of a signal is not well enough predicted. The worst situation is obviously when the predicted signal and the actual one are completely out of phase, that is to say when the phase difference between both signals is  $180^\circ$ . In that particular situation, the true signal and the predicted one have opposite signs. Disregarding any notion of frequency, it is interesting to divide the predicted signal in two parts. The first part (the "good" one), is when the predicted signal has same sign as the true signal and the second part (the "bad" one), is when the predicted signal has a sign opposite to the sign of the true signal. The relative importance of both parts gives a rough idea of the quality of the prediction. To make things more precise, let us consider (see figure 2), two sinusoidal signals with the same frequency. The solid red line is the signal of reference and the large solid blue line is the supposedly predicted signal. The second signal is time shifted

in comparison to the the reference signal in red. The blue signal is decomposed in two parts, the green dotted part and the black dotted one. The green dotted part is equal to the blue signal when this one has same sign as the red signal of reference and is zero otherwise. The black dotted part is equal to the blue signal when this one has a sign opposite to the sign of the red signal of reference and is zero otherwise. So the blue signal is equal to the sum of the green dotted ("good" part) and black dotted ("bad" part) signals. The relative importance of the two parts, the "good" and "bad" ones, is directly related to the phase shift. For a reference signal which is not mono-chromatic, it is still possible to make a power spectrum analysis and compare the relative importance of the two parts of the decomposition for any given frequency. Of course, the sharp transitions, occurring in the two parts resulting from the decomposition of the predicted signal, introduce harmonics in the frequency analysis. This is why this tool can only be a crude one. Nevertheless, as the amplitude of the harmonics is less than the amplitude of the fundamental, they will not bias too much the interpretation of the results. The application of this test to the experiment is presented in figure 4. On this particular example, the "bad" part of the reconstructed signal is always negligible when compared to the "good" part. This gives us at least some hope that unwanted instabilities may be avoided when the active control feed-back loop is designed. We can also note that for the 122.7 Hz mode, which is conspicuous on channels 4, 5 and 6, the identified signal has only half the energy which is present on the experimental signal. This is not surprising because we don't have excitation over 100 Hz as we have seen in figure 3. The identified part has nevertheless the correct phase.

### 5.2 Second tool to check validity of the results.

We will now introduce another tool for the analysis of the results. This second tool is more precise than the first one but the very convenient comparison with the power spectrum of the experimental signal is not possible. Let us consider the case of constant systems (no time variations). Particularly when we have many inputs, it is not the detailed comparison (in modulus and phase) of the measured and reconstructed transfer functions for each input which is important. What is important for active control, is the phase between the experimental signal and the reconstructed one at each frequency in the range of interest. There is one simple function which gives such a result. It is the transfer function using the reconstructed signal as output and the measured signal as input. The modulus of such a transfer function should be close to 1 and its phase close to zero for an excellent reconstruction of the experimental signal. Of course, important phase errors are not a problem when the signals are very weak, that is to say for frequencies where the power spectra are small. So the transfer function between the

reconstructed and experimental signal must be interpreted in conjunction with the power spectra of the experimental and reconstructed signals. The first tool may supply that kind of information. Both tools are thus complementary.

For a periodic system the inputs are multiplied and the outputs must be reconstructed according to formula (1) but the analysis given by the second tool retains all its value. The application of this test to the identification of the model is presented in figures 5-a and 5-b.

## 6. COMMENTS ON THE RESULTS OF THE IDENTIFICATION

The identification is made by the method of Mäkilä as explained earlier.

The results are presented in figures 3-4-5. As we have 3 independent inputs, this case is very complex as far as the computation is concerned. We have  $3 \times 60 = 180$  inputs for each revolution of the rotor. The shortest time history of the input necessary for a good identification of the outputs is 12 revolutions of the rotor. Then, 12 matrices with size  $60 \times 180$  have to be determined for each output channel. In spite of the difficulty of the problem, the results which have been obtained are in fact very good. The power spectra of the experimental and identified signals are presented in figure 4. On this figure, the abscissas are the frequencies in reduced form, the value 1 corresponds to 200 Hz because the sampling frequency is 400 Hz. We have 12 channels in figure 4, the first 9 channels are from signals coming from the gauges or angular transducers on the rotor and the last 3 channels are for the displacement transducers located on the actuators. This last 3 transducers are located into the non rotating frame and they don't necessitate a periodic system analysis. Nevertheless a time invariant system may also be considered as a particular case of periodic system and the same analysis has been applied to all the channels. Still, on channels 10, 11, 12 the results are better because the system to be identified is simpler.

As the 3 input signals have been registered, these signals are used to compute the responses of the identified system. The power spectra of the computed responses may be compared to the power spectra of the measured responses.

Generally the two power spectra are in good agreement though obviously not all the details are retained by the identification. We still have to check the validity of the results with the two tools at our disposal.

First, the reconstructed signals are divided into two parts. The first part with same sign as the experimental signal and the second part with a different sign. The power spectra of both parts are presented in figure 4. As may be seen on this picture the part with a sign opposite to the experiment (the "bad" part) is barely visible. This is already a good indication of the validity of the results. However, on channels 4, 5 and 6, the

pick at 122 Hz is not entirely found and this is not surprising. There is no input at this frequency as may be seen in figure 3 channels 13, 14, 15. The physical input, if any, must then be the noise generated by the mechanical shocks in the command chain.

The quality of the results is confirmed by the second tool, the transfer function between the reconstructed and experimental signals (figures 5–a and 5–b).

The frequency range of interest is from 0 to 100 Hz that is to say from 0 to 0.5 in reduced form. In the frequency range of interest, the phase of the transfer function is always less than 10 degrees. This phase is particularly small for the channels 10, 11, 12, that is to say for the actuators which are in the non rotating part of the structure.

Let us now look at the modulus of the transfer functions. As was explained earlier, this modulus should be equal to 1 if the identification was perfect. As may be seen in figures 5–a and 5–b, we are far from that. On channels 10, 11 and 12, the results are perfect up to 80 Hz (reduced frequency 0.4). These transducers are in the non–rotating frame and up to 80 Hz there is a good level for the inputs. Over 80 Hz the results deteriorate. For the response on the strain gauges at mid–distance from the tip of the blade (Channels 7, 8, 9), the results are also quite acceptable in the frequency range 0–80 Hz. For the other transducers the variations of the transfer function modulus are larger. Still, the modulus remains close to 1 when the level of the response is important, that is to say when we are close to the resonant frequencies. It is also remarkable, in figure 5, that the modulus on all the channels, remain always less or equal to 1. This means that the identification predicts signals always of smaller amplitude than the experimental ones. The predicted and measured signals are almost in phase. Is this enough to assure stability of the control loop ? There is no general response to this question. One can guess that if the identification underestimate the responses, the control loop may try to overcompensate. This may increase the vibrations. Of course, it is always possible to multiply the matrices into the identification formula (1) by a real coefficient greater than 1. The phase would remain the same and the predicted amplitude would be larger. The control loop would then be less prone to overcompensation but also probably at the price of a lesser efficiency.

## 7. CONCLUSION.

The identification of the Edy rotor model which has been experienced in the BRAVoS test rig was a difficult task. As the identification of the model was tempted on a rather large frequency band, the number of points by rotation is high (60 points). The number of coefficients to be determined is then

also very large. Moreover, the maximum frequency of the input is limited to 100 Hz for fear of instabilities in the hydraulic actuators but all the signals are discretized with a recording frequency of 400 Hz. Thus, the inputs cannot be entirely independents and the identification cannot be unique. The solution must be researched by the SVD (Singular Value Decomposition) technique (reference [6]) and this is a problem for the numerical stability of the code. In spite of all the difficulties, the identification of multi–input, multi–output periodic systems is now operational. The method of identification has been extended by the introduction of two tests for the checking of the validity and accuracy of the identified system. This tests, applied to the present results have shown that the rotor model has been accurately identified.

The identification, as it is proposed in the present report, furnishes systems much too clumsy for the design of control loops by usual methods. Nevertheless other methods, simulations, LMS (Least Mean Square) or IMC (Internal Model Control) may be used.

## 8. REFERENCES.

- [1] **Moonen M. , De Moor B. , Vandenberghe I. , Vandewalle J. :** *On– and off–line identification of linear state–space models.* International Journal of Control. Vol. 49 , Nb. 1 , January, 1989
- [2] **Hench J.J. :** *robustA technique for the identification of linear periodic state–space models.* International Journal of Control. Vol. 62 , Nb. 2 , August, 1995
- [3] **Mäkilä P.M :** *On robust–oriented identification of discrete and continuous–time systems.* International Journal of Control. Vol. 70 , Nb. 2 , May 20, 1998
- [4] **Mäkilä P.M :** *State space identification of stable systems.* International Journal of Control. Vol. 72 , Nb. 3 , February 15, 1999
- [5] **Costes J.J Legrain–Naudin I.:** *Design of a feedback active control regulator for reduction of vibrations or noise in a helicopter cabin.* 25th European Rotorcraft Forum . Roma (Italy), September 14–16, 1999.
- [6] **Press W.H. Flannery B. P. Teukolsky S. A. Vetterling W. T.:** *Numerical Recipes. The art of scientific computing.* Cambridge University Press 1989.



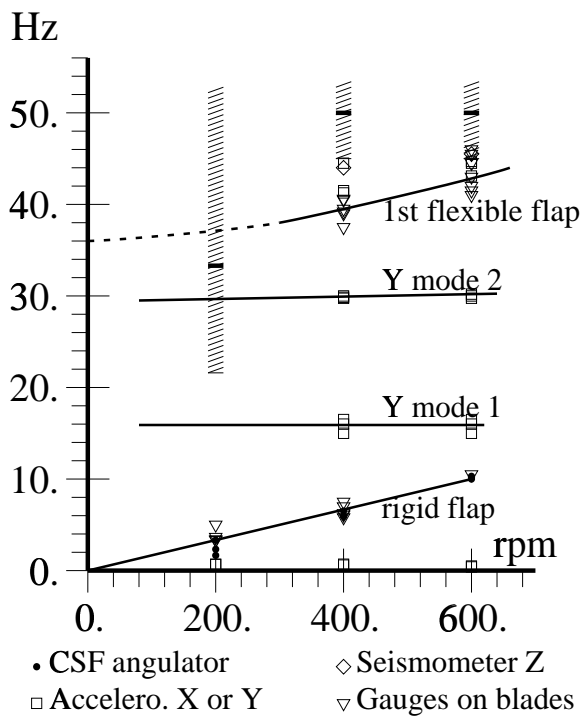


figure 1 : Measured resonant frequencies (rigid setting case).

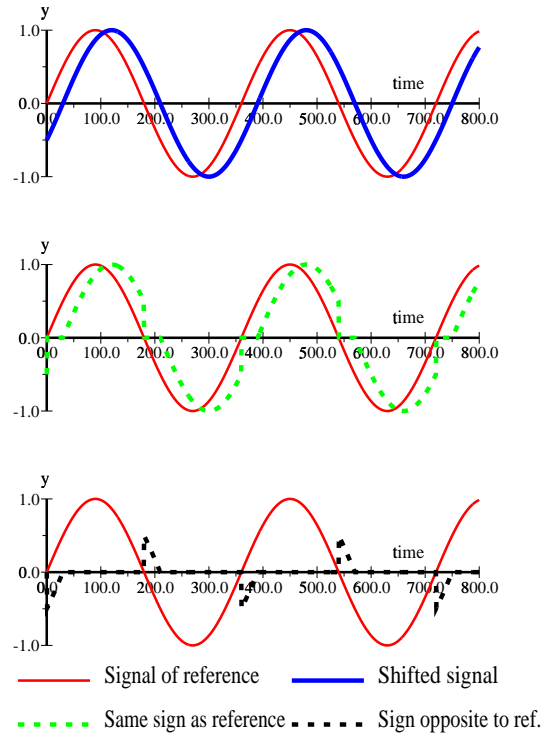
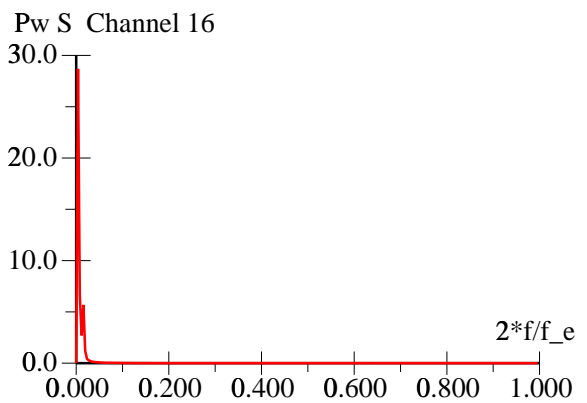
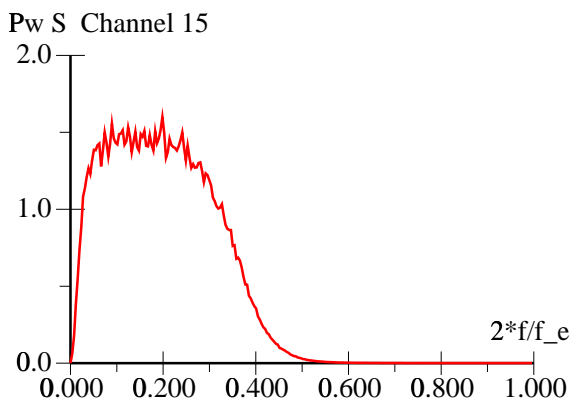
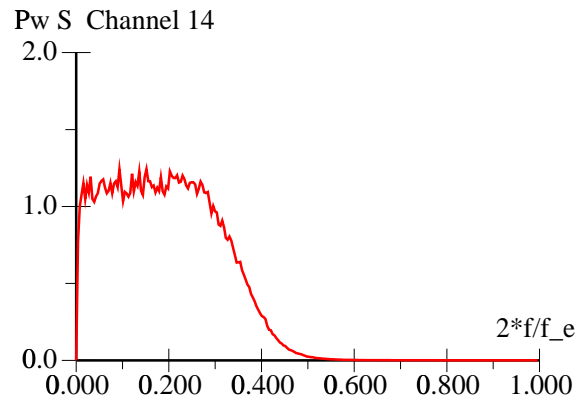
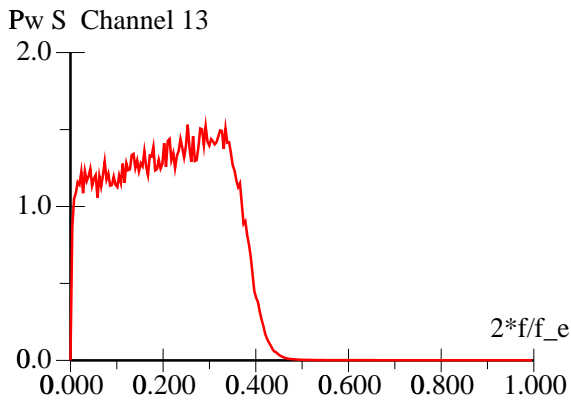
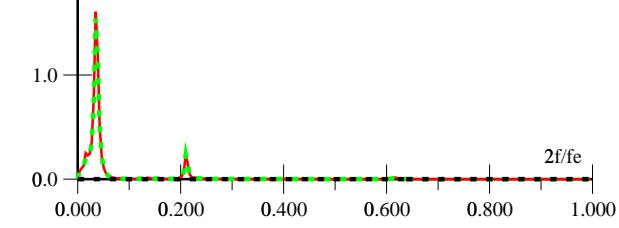


figure 2: Analysis by decomposition of a time shifted signal.

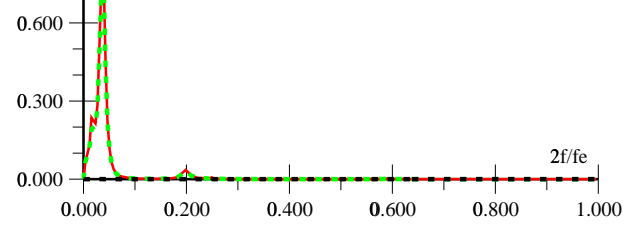
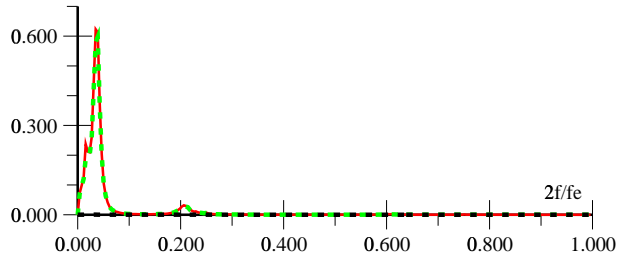


— Experiment

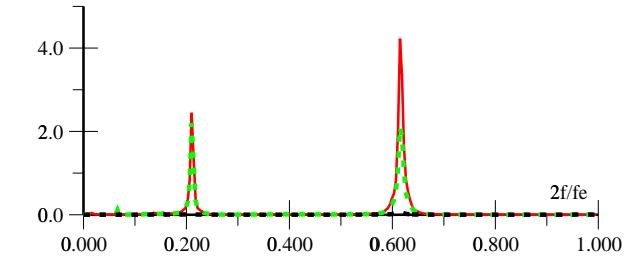
figure 3 : Power spectra of the experimental signals.



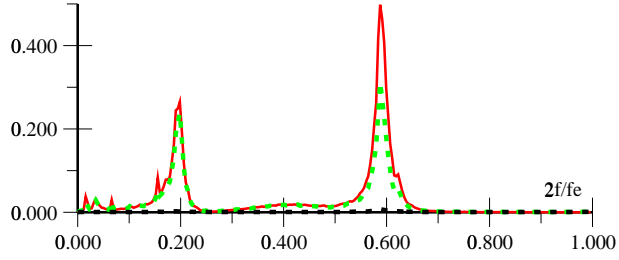
Pw. S. Channel 3



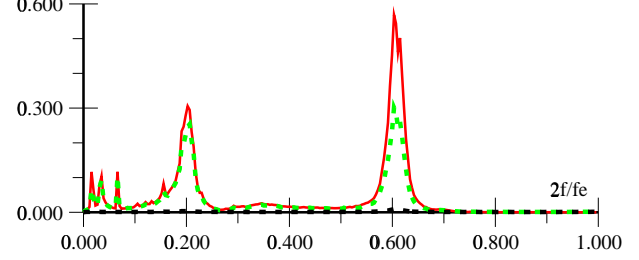
Pw. S. Channel 4



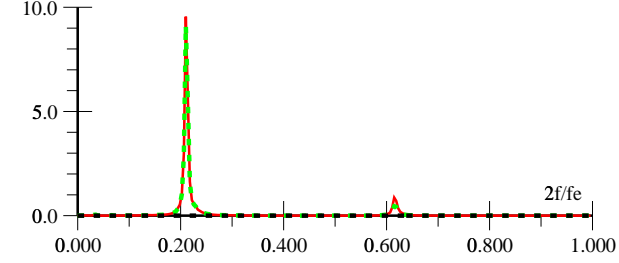
Pw. S. Channel 5



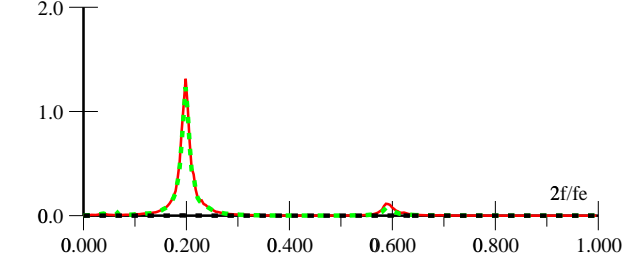
Pw. S. Channel 6



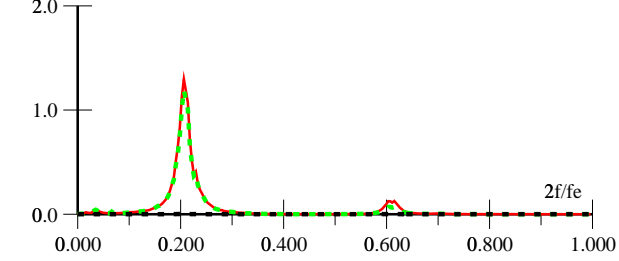
Pw. S. Channel 7



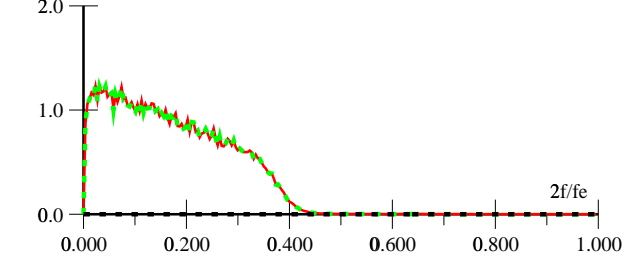
Pw. S. Channel 8



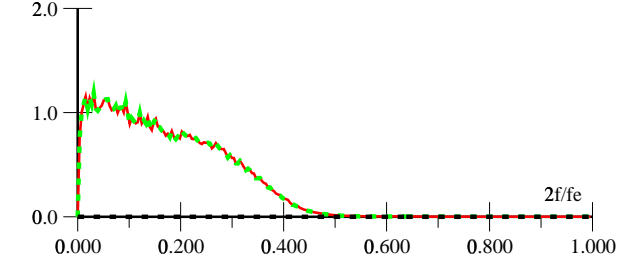
Pw. S. Channel 9



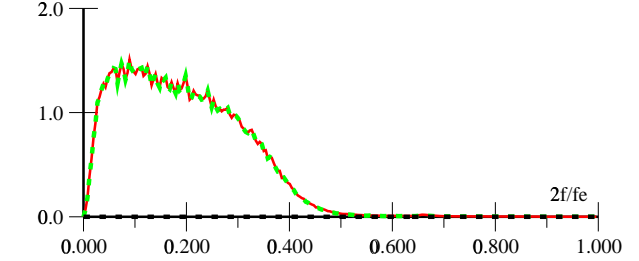
Pw. S. Channel 10



Pw. S. Channel 11

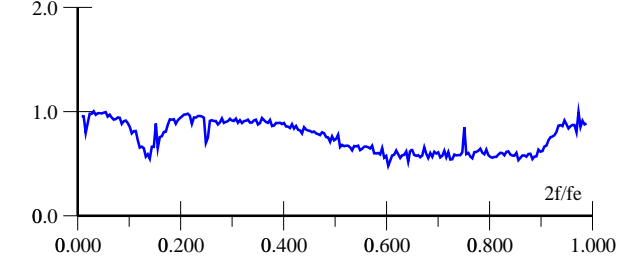


Pw. S. Channel 12

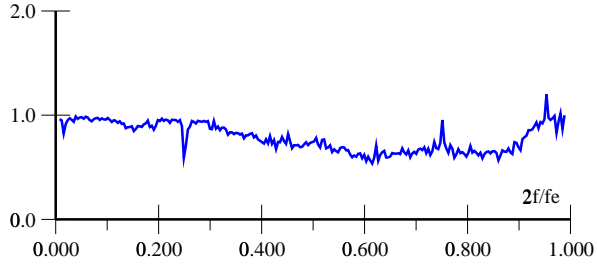


————— Experiment  
- - - - - Identif. same sign as exp.  
- - - - - Identif. sign opposite to exp.

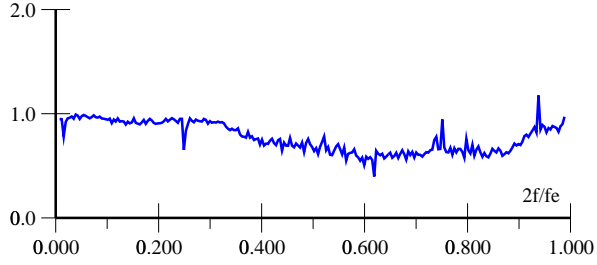
figure 4: Analysis by decomposition of the power spectra



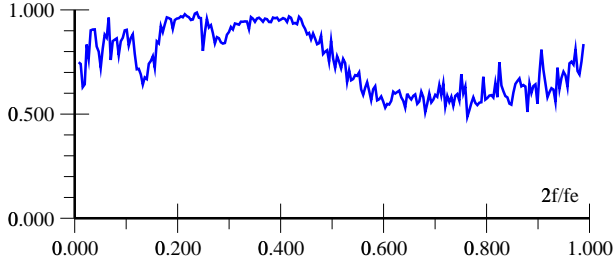
modulus TF. Theory/Expe. Channel 2



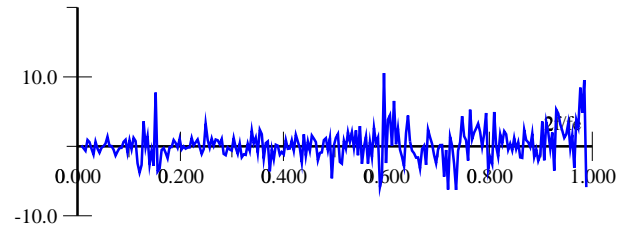
modulus TF. Theory/Expe. Channel 3



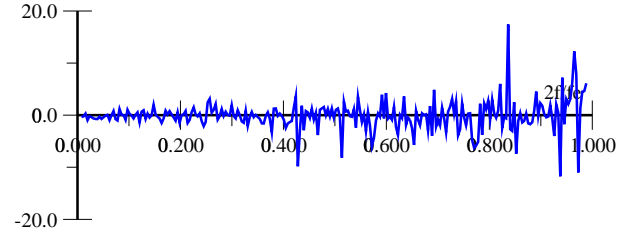
modulus TF. Theory/Expe. Channel 5



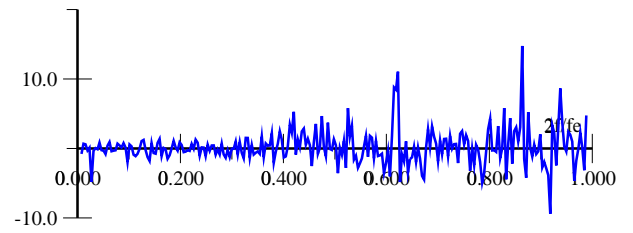
modulus TF. Theory/Expe. Channel 2



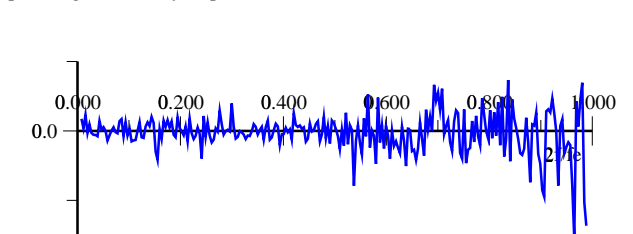
phase dg TF. Theory/Expe. Channel 3



phase dg TF. Theory/Expe. Channel 4



phase dg TF. Theory/Expe. Channel 5



phase dg TF. Theory/Expe. Channel 6

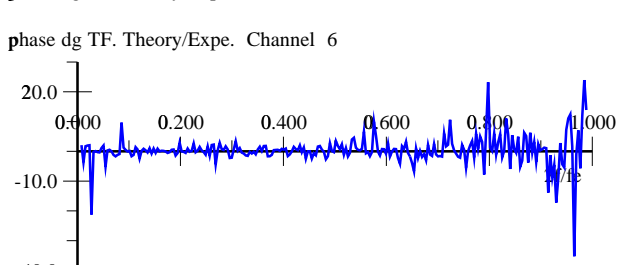


figure 5-a: Transfer function (Modulus and Phase)

Experiment as input and Theory as output.

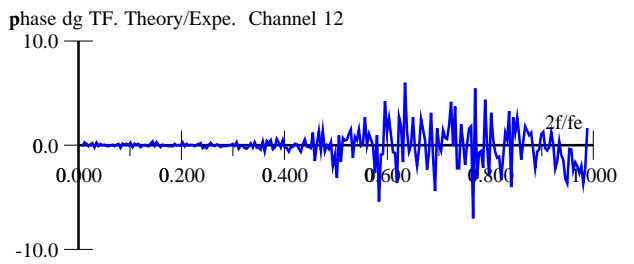
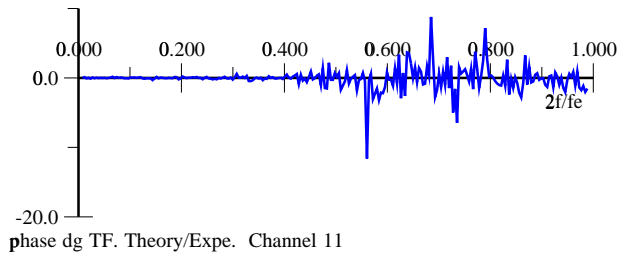
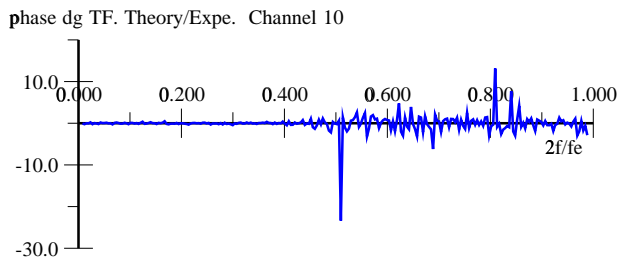
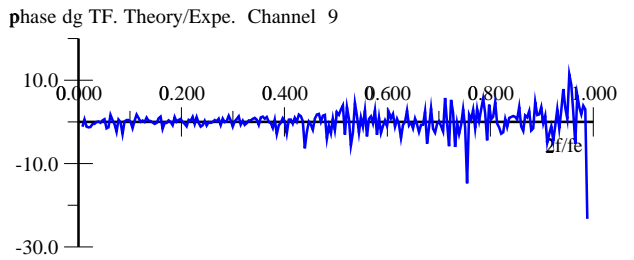
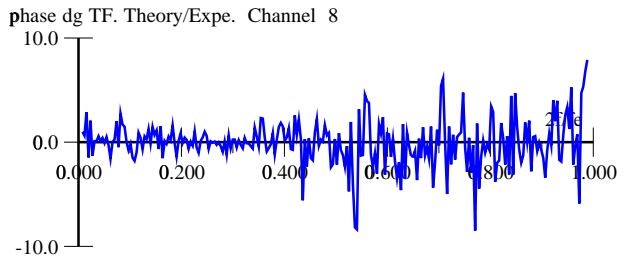
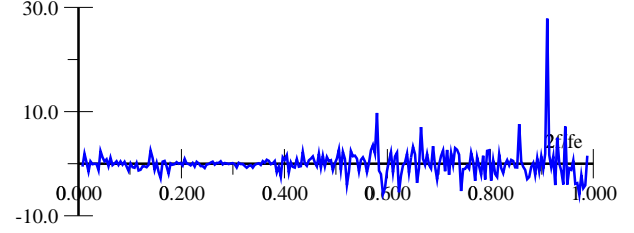
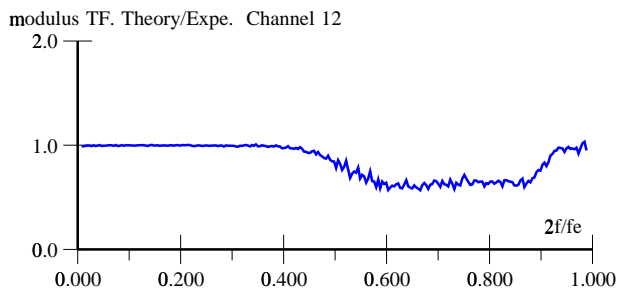
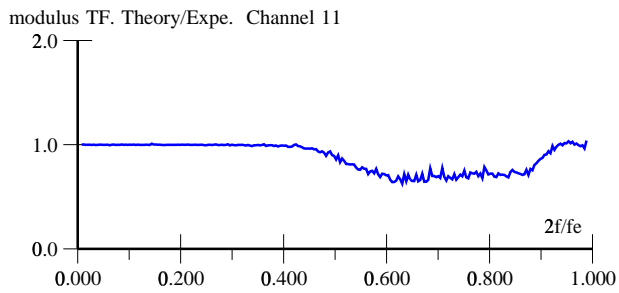
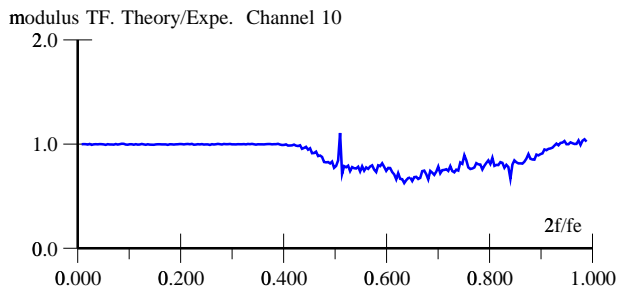
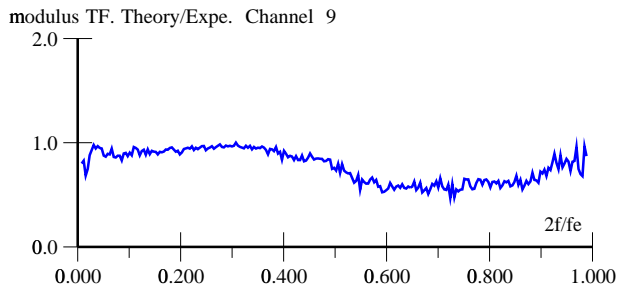
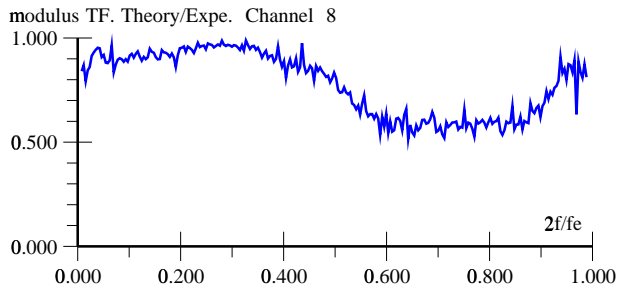
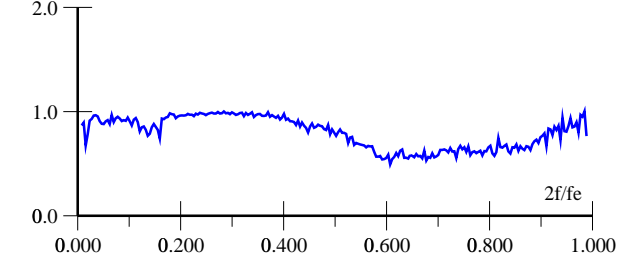


figure 5-b : Transfer function (Modulus and Phase)

Experiment as input and Theory as output.